Inorganic Chemistry

Article

pubs.acs.org/IC

Substantial Cd−Cd Bonding in Ca_6PtCd_{11}: A Condensed Intermetallic Phase Built of Pentagonal Cd_7 and Rectangular $Cd_{4/2}Pt$ Pyramids

Fakhili Gulo,† Saroj L. Samal, and John D. Corbett*

Ames Laboratory, DOE and Department of Chemistry, Iowa State University, Ames, Iowa 50010, United States

Supporting Information

ABSTRACT: The novel intermetallic Ca_6PtCd_{11} is orthorhombic, *Pnma*, $Z = 4$, with $a = 18.799(2)$ Å, $b = 5.986(1)$ Å, $c = 15.585(3)$ Å. The heavily condensed network contains three types of parallel cadmium chains: apically strongly interbonded Cd_7 pentagonal bipyramids, linear Cd arrays, and rectangular $Cd_{4/2}Pt$ pyramids. All of the atoms have 11−13 neighbors. Calculations by means of the linear muffin-tin orbitals method in the atomic spheres approximation indicate that some Cd−Cd interactions correspond to notably high Hamilton populations (1.07 eV per average bond) whereas the Ca−Ca covalent interactions (integrated crystal orbital Hamiltonian population) are particularly small (0.17 eV/bond). (Pt−Cd interactions are individually greater but much less in aggregate.) The Ca−Ca separations are small, appreciably less than the single bond metallic diameters, and unusually uniform ($\Delta = 0.14$ Å). The Cd atoms make major contributions to the stability of the phase via substantial 5s and 5p bonding, which include back-donation of Cd 5s, 5p and Pt 5d into Ca 3d states in the principal bonding modes for Ca−Cd and Ca−Pt. Bonding Ca−Ca, Ca−Cd, and Cd−Cd states remain above E_F, and some relative oxidation of Ca in this structure seems probable. Ca_6PtCd_{11} joins a small group of other phases in which Cd clustering and Cd−Cd bonding are important.

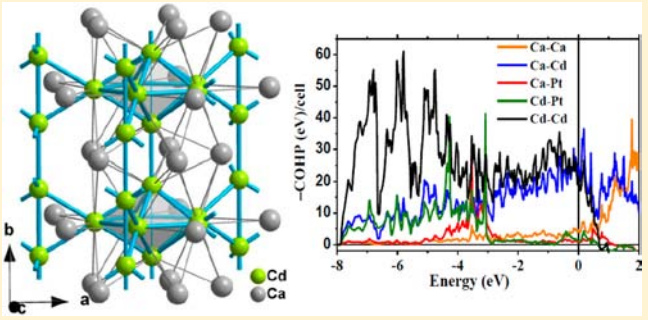

INTRODUCTION

Exploratory syntheses in intermetallic systems have led to numerous novel compounds with unprecedented structures and unusual bonding features.[1] To understand and rationalize this rich chemistry and its associated complex bonding remains extremely challenging. Polar intermetallic phases formed between alkali metals or alkaline-earth metals and multiple heavy p-block elements often qualify as Zintl (valence) phases, which attain closed-shell electron configurations through formal electron transfer and covalent closed-shell bond formation.[2−5] The more recent utilization of earlier p-metals and, often, late transition metals as well has led to many new electron-poorer yet strongly bonded products with new structural features. Such compounds are electronically situated between Zintl and Hume−Rothery phases and often entail more highly condensed structures and fewer valence electrons per atom (e/a). Gold in particular has been very effective in affording new and unusual clusters, networks, or tunnel constructions with a range of cations, evidently because of substantial relativistic effects[6] that enhance gold's bonding to itself and later metals, for example, in many A/Ae−Au−Tr/Tt systems (A = alkali metal, Ae = alkaline earth metal, Tr = triel (Ga, In, Tl), Tt = tetrel (Ge, Sn)).[7−15] Introduction of late transition metals such as Cd and Zn in place of Tr leads to larger clusters and more networks. For example, we recently discovered gold-based ternary compounds such as $Na_6Au_7Cd_{16}$ built on cadmium tetrahedral stars[16] and a greatly contrasting Na−Au−Zn system with tunnel structures populated by somewhat diffuse but locally ordered cation distributions.[17] Switching the electropositive component to the more tightly bound alkaline-earth or rare-earth (R) metals generally produces higher symmetry phases and more uniform packing.[18]

Relatively few studies have been carried out on the neighboring platinum-based ternary intermetallic systems[19−22] although some amount of gold's novel relativistic enhancement of bonding would seem likely for Pt. Most studies have pertained mainly either to higher cation or Pt proportions or to products unrelated to those in the present study.

Enhancements of the cadmium proportions in such ternaries have been found to yield phases with new and novel aggregations of this component. Recently, we reported $Ca_6Pt_8Cd_{16}$,[23] which contains strongly bonded Pt-centered calcium octahedra ($Pt@Ca_6$) and a network of Cd_8 tetrahedral stars that are face-capped by Pt. Nearly the same arrangement is also found in the close Na−Au analogue $Na_6Au_7Cd_{16}$[16] as well as in $Er_6Sb_8Pd_{16}$, a provocative *inverse* relative of the first analogue.[24] These structures seem to be dominated by strongly interbonded T−Cd aggregates in which T refers to a late, heavy transition metal Au, Pt, Pd, etc., whereas Cd seemingly lacks a competitive condensed cluster chemistry of its own in the

Received: June 8, 2013
Published: August 19, 2013

   dx.doi.org/10.1021/ic401455c | *Inorg. Chem.* 2013, 52, 10112−10118

presence of much T and lower-valent alkali metals or alkaline-earth metals.

Here we report a novel contrary example, the monoplatinide Ca_6PtCd_{11}, in which a significant pseudouniaxial Cd network is also bridged by a small number of pyramidal $PtCd_{4/2}$ units, and these are all enveloped by a Ca array. The presence of higher proportions of calcium and cadmium and the relatively strong homoatomic bonding characteristics for cadmium give rise to a new network based on chain and cluster formation. Only a small number of other distant cadmium compounds show any suggestions of significant cadmium cluster chemistry.

EXPERIMENTAL SECTION

Synthesis. Starting materials for the syntheses were dendritic calcium (99.9%, Alfa Aesar), platinum (99.995%, Lonmin), and cadmium (99.99%, Alfa Aesar). The new product was initially isolated from an exploratory Ca_2PtCd_2 composition, after which an X-ray pure sample was synthesized from a stoichiometric mixture of the components. The elements were weighed (±0.1 mg) and enclosed in a tantalum tube in a nitrogen-filled glovebox (H_2O < 0.1 ppm by volume), weld-sealed under argon, and then enclosed in an evacuated silica jacket to protect the tantalum from air oxidation. The samples were reacted at 950 °C for 15 h, quenched in water, equilibrated at 600 °C for 4 days, and then slowly cooled to room temperature. Ca_6PtCd_{11} is brittle, silver-gray in color, and visually inert to air at room temperature for at least several days. Attempts to synthesize Sr, Ba, Au, or Pd analogues were unsuccessful.

Ca_6PtCd_{11} is regularly obtained in the cadmium-rich region of the ternary system. However, if the sample is quenched from ∼950−1000 °C, the high-temperature form of $CaCd_2$[25] (KHg_2, *Imma*) is obtained along with ∼15% of an unknown phase (Supporting Information, Figure S3), but annealing at 600 °C recovers the new 6-1-11 phase quantitatively. The title compound is evidently very close to a line phase as no lattice constant evidence for significantly mixed or partial site occupancies could be induced by compositional variations in its syntheses ($Ca_6Pt_xCd_{12-x}$ for x = 0.75, 1.5, 2). Attempts to gain an analogous Zn compound always yielded the parent orthorhombic $CaZn_2$-type structure[26] isostructural with high-temperature $CaCd_2$ but with a mixed Zn/Pt site.

X-ray Diffraction Studies. Powder diffraction data were collected at room temperature with the aid of a Stoe Stadi P powder diffractometer equipped with an image plate and Cu Kα radiation (λ = 1.54059 Å). The samples were dispersed between two acetate films with the aid of a little grease and sealed in the Stoe airtight sample holder by means of a metal cover seated by screws. The lattice parameters were refined using the WinXPow program,[27] and all the distance calculations from single crystal data used these values.

Diffraction data sets were collected at room temperature over a 2θ range of ∼3° to ∼57° as three sets of 606 frames with 0.3° scans in ω and 10 s per frame exposures with the aid of a Bruker SMART CCD diffractometer equipped with Mo K_α radiation (λ = 0.71073 Å). The reflection intensities were integrated with the SAINT program in the SMART software package.[28] Empirical absorption corrections were made with the aid of the SADABS program.[29] Determination of the space group as *Pnma* was accomplished with the aid of XPREP and SHELXTL 6.1.[30] The structure was solved by direct methods and subsequently refined on $|F^2|$ with a combination of least-squares refinements and difference Fourier maps.

Systematic extinctions indicated a primitive orthorhombic lattice with two glide conditions, and the Ca_6PtCd_{11} structure was solved and well refined in *Pnma*. The final refinement with anisotropic displacement parameters converged to R_1 = 0.0351, wR_2 = 0.0517 for all data with a goodness-of-fit on F^2 of 0.98 and density residuals that were ≤1.2 e Å^{-3}. Details of data collection and structure refinements are in Table 1, and the atomic positions and equivalent isotropic displacement parameters are in Table 2. Anisotropic displacement factors and all near-neighbor interatomic distances (and integrated crystal orbital Hamiltonian population (ICOHP) data) are in Supporting Information, Tables S1 and S2, respectively, along with the CIF file. Single standard deviations of occupancy refinements limit the mixing of Ca into Cd sites and of Cd into Ca sites to less than 0.7% and 0.9%, respectively.

Table 1. Crystal Data and Structure Refinement for $Ca_6Cd_{11}Pt$

empirical formula	$Ca_6Cd_{11}Pt$
formula weight	1671.97
space group, Z	*Pnma*, 4
unit cell dimensions	a = 18.799(2) Å, b = 5.986(1) Å, c = 15.585(3) Å
volume	1772.2(6) Å^3
density (calculated)	6.266 Mg m^{-3}
absorption coefficient	22.462 mm^{-1}
theta range for data collection	2.16−28.25 deg.
index ranges	$-24 \le h \le 25$; $-7 \le k \le 7$; $-20 \le l \le 20$
reflections collected	11799
independent reflections	1934 [R_{int} = 0.0417]
data/restraints/parameters	1934/0/100
goodness-of-fit on F^2	0.987
final R indices [I > 2σ(I)]	R_1 = 0.0259; wR_2 = 0.0499
R indices (all data)	R_1 = 0.0351; wR_2 = 0.0517
largest difference peak and hole	1.187 and −0.910 e.Å^{-3}

Electronic Structure Calculations. Tight binding calculations for Ca_6PtCd_{11} were performed according to the linear muffin-tin orbital (LMTO) method in the atomic sphere approximation (ASA).[31] The radii of the Wigner−Seitz spheres were assigned automatically so that the overlapping potentials would be the best possible approximations to the full potentials.[32] No additional empty sphere was needed subject to an 18% overlap restriction for atom-centered spheres. The radii were Ca1 = 2.08 Å, Ca2 = 2.08 Å, Ca3 = 1.96 Å, Ca4 = 1.95 Å, Ca5 = 2.08 Å, Ca6 = 2.08 Å, Cd1 = 1.69 Å, Cd2 = 1.69 Å, Cd3 = 1.69 Å, Cd4 = 1.69 Å, Cd5 = 1.69 Å, Cd6 = 1.70 Å, Cd7 = 1.69 Å, Cd8 = 1.64 Å, and Pt = 1.43 Å. The basis sets employed included Ca 4s, 3d, (4p); Cd 5s, 5p, (4f); and Pt 6s, 6p, 5d, (5f) (downfolded orbitals in parentheses), and the reciprocal space integrations were carried out using the tetrahedron method. The Cd 4d states were considered to be core electrons because these lie far below the Fermi level, but they also result in significant artificial Cd 4d−Pt 5d coupling if not omitted. Scalar relativistic corrections were included; these contributed 6−19% of the total ICOHP values per bond. For bonding analysis, the energy contributions of all filled electronic states for selected atom pairs were calculated by the crystal orbital Hamilton population (COHP) method,[33] and the energy-weighted ICOHP sums up to E_F for each bond type were also calculated as Hamilton populations, which are approximations of relative bond orders. The results are in the Supporting Information, Table S2.

RESULTS AND DISCUSSION

The Structure. New polar intermetallics with all of their variety frequently provide pleasant surprises in the form of unusual complex structures and novel bonding patterns. Replacement of 1/12 of the Cd atoms in the parent Laves phase $CaCd_2$ by Pt results in a quantitative yield of the unprecedented Ca_6PtCd_{11}. The heavily networked anionic (Cd, Pt) portion of orthorhombic Ca_6PtCd_{11} (*Pnma*, Z = 4; a = 18.799(2) Å, b = 5.986(1) Å, c = 15.585(3) Å) is viewed in Figure 1a almost along the short b axis and the three defining Cd chains. These consist of (1) strongly interbonded pentagonal bipyramidal (PBP) Cd_7 clusters (green atoms and gray pentagons), (2) interbonded linear Cd3 chains, and (3) a smaller proportion of parallel trans-edge-sharing rectangular pyramidal $Cd_{4/2}Pt$ clusters (with orange Pt). The first two units

dx.doi.org/10.1021/ic401455c | *Inorg. Chem.* 2013, 52, 10112−10118

Table 2. Atomic Coordinates and Equivalent Isotropic Displacement Parameters for $Ca_6Cd_{11}Pt$

atom	Wyckoff position	site symmetry	x	y	z	U_{eq} [Å^2][a]
Cd1	8*d*	1	0.1096(1)	0.5001(1)	0.4565(1)	0.0134(1)
Cd2	8*d*	1	0.1809(1)	0.0155(1)	0.1509(1)	0.0146(1)
Cd3	8*d*	1	0.4090(1)	0.0034(1)	0.3369(1)	0.0169(1)
Cd4	4*c*	m.	0.2008(1)	1/4	0.7431(1)	0.0161(2)
Cd5	4*c*	m	0.2151(1)	1/4	0.5526(1)	0.0125(1)
Cd6	4*c*	m	0.3529(1)	1/4	0.8037(1)	0.0139(1)
Cd7	4*c*	m	0.3664(1)	1/4	0.4957(1)	0.0149(2)
Cd8	4*c*	m	0.4567(1)	1/4	0.6562(1)	0.0160(2)
Ca1	4*c*	m	0.0346(1)	1/4	0.6268(1)	0.0166(4)
Ca2	4*c*	m	0.0427(1)	1/4	0.0391(1)	0.0164(4)
Ca3	4*c*	m	0.0489(1)	1/4	0.2741(1)	0.0146(4)
Ca4	4*c*	m	0.2408(1)	1/4	0.3376(1)	0.0157(4)
Ca5	4*c*	m	0.3499(1)	1/4	0.1463(1)	0.0147(4)
Ca6	4*c*	m	0.7263(1)	1/4	0.5399(1)	0.0161(4)
Pt1	4*c*	m	0.4846(1)	1/4	0.0572(1)	0.0138(1)

[a] U_{eq} is defined to be one-third of the trace of the orthogonalized *Uij* tensor.

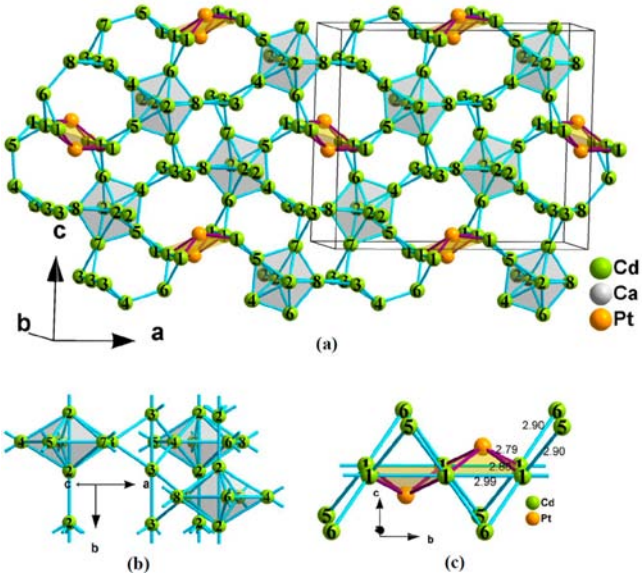

Figure 1. Approximate (010) view of the anionic structure of $Ca_6Cd_{11}Pt$ (*Pnma*) along the *b* axis. (a) The anionic part contains Cd_7 pentagonal bipyramids (green atoms with gray polyhedra), three of which are interconnected via a Cd3 chain and a pair of edge-shared $Cd_{4/2}Pt$ chains at the four waist centers of the cell. The latter interconnect four Cd_7 PBP clusters in a trans configuration. (b) Three Cd_7 PBP clusters interconnected via chains of Cd3 atoms, one of the former being displaced by *b*/2. (c) A pair of edge-shared $Cd_{4/2}Pt$ clusters with Pt in apical positions. The independent Cd−Pt and Cd−Cd distances are marked.

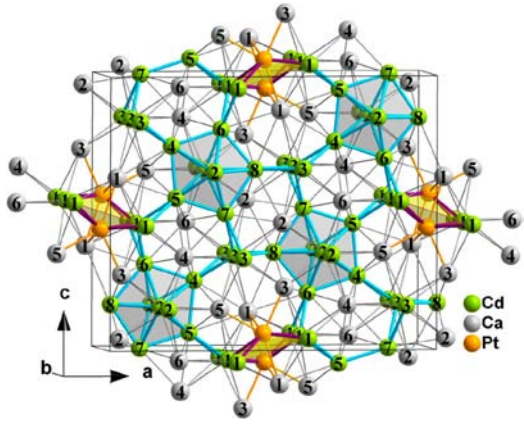

Figure 2. Approximate (010) section of the structure of $Ca_6Cd_{11}Pt$. Only the (gray) cations that lie within this section are shown.

are also shown in a clarified side view in Figure 1b and the third in Figure 1c. Further Cd−Cd and Cd−Pt interchain bonding connects these into a 3D network along the *b* axis (Figure 1a) that is ultimately surrounded by and bonded to a cationic array of gray Ca atoms (Figure 2).

To complete the anionic network, each Cd_7 PBP is connected to two identical trans clusters through shorter axial Cd2−Cd2 bonds to form infinite chains along the *b* axis. Three such Cd_7 chains are further interconnected along the *b* axis via a linear chain of unevenly spaced Cd3 atoms in such a way that two adjacent PBP clusters are coplanar, and a third is displaced by *b*/2 (Figure 1b). The oblate Cd_7 clusters have approximate D_{5h} symmetry with internal Cd−Cd edges in the range of 2.99 ± 0.09 Å and bond angles of 108 ± 5°. The axial intercluster Cd2−Cd2 bond length between the PBP, 2.807(1) Å, is the shortest, and others range up to 3.09 Å, whereas the internal (trans) Cd2−Cd2 distance in the already compressed bipyramid is longer, 3.179(1) Å. Significant cation "solvation" is evidently responsible for some of these distortions (see below). Likewise, a chain of shared rectangular Cd1 units capped by well-bonded apical Pt atoms (orange) are the basis for parallel chains of trans-edge-sharing rectangular pyramids ($Cd_{4/2}Pt$) along the *b* axis that are centered on four cell faces: 0 1/2 1/2 and 1/2 1/2 0, etc. (Figure 1a,c). (The shared Cd−Cd edges lie on inversion centers, and successive platinum vertices fall on alternate sides of the chain.) Pairs of Cd1 atoms on the backside of this chain (Figure 1c) are also bonded through Cd5 and Cd6 vertexes to four different PBP strings in a trans configuration (Figure 1a). The overall impression is that of a heavily interlinked 3D anionic array of PBP Cd atoms pinned by about 10% as much Pt in parallel Cd chains along the *b* axis. More about the independent Cd−Cd and Cd−Ca interactions per cell and the apparently very good "fit" of the structure will be considered later in bonding analyses.

The Ca cations (Figure 2 and Supporting Information, Figure S2) are dispersed in the three types of open tunnels along the *b* axis (Figure 1a) so as to surround the anionic

dx.doi.org/10.1021/ic401455c | *Inorg. Chem.* 2013, 52, 10112−10118

components. The most striking interactions involve their "solvation" of the PBP units (Figure 3a). Each Cd7 cluster

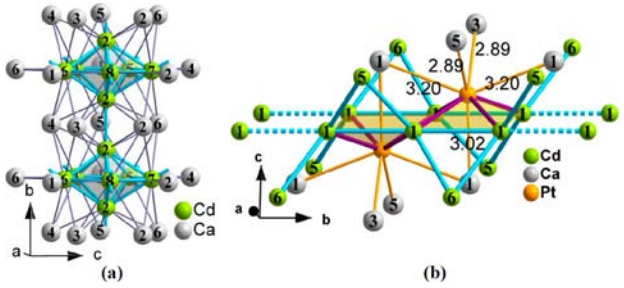

Figure 3. (a) A pair of Cd_7 pentagonal bipyramids encapsulated in a Ca_{25} cage continue as a chain along the *b* axis. (b) A pair of $Cd_{4/2}Pt$ square pyramids with all Ca−Pt bonds marked. The shared Cd−Cd edges contain inversion centers so that platinum occupies apical positions on alternate sides.

(yellow) is bonded to 15 nominal surface cations that lie over its 10 trigonal faces and also bridges the five waist edges of the PBP. The five face-capping atoms Ca 2, 3, 4, 5, and 6 around each Cd2−Cd2 boundary in fact cap all 10 faces on both adjoining PBP, and so on along the whole chain. This certainly must be the reason for the exceptionally short (2.807 Å) Cd2−Cd2 bonds and, inferentially, the stability of the pentagonal chains (Figure 3a). Each of these capping Ca atoms is also bonded to four or five Cd atoms on the back side of the array. (A more inclusive view with Cd1 chains appears in the Abstract figure above.) The $Cd_{4/2}Pt$ rectangular pyramids are also surrounded by a total of 15 shared Ca atoms that cap faces or edges or are exo-bonded (Figure 3b and Supporting Information, Figure S2). Of particular note are the four short Pt−Ca interactions: Ca5 at 2.887(2) Å, Ca3, 2.894(2) Å, and Ca1, 3.019(2) Å (x2) on the Pt side and a similar 3.024(1) Å Ca1 contact at the back. All exhibit appreciable Pt 5d−Ca 3d bonding (see below).

Finally, the naturally longer and less covalent Ca−Ca contacts (see below) occur over a quite narrow (~0.14 Å) range, 3.603(2)−3.742(3) Å throughout this complex structure, a significant and moderately uniform "floating" distribution (Supporting Information, Table S2; one or two outlying atoms are omitted). The Ca−Cd distances in the present structure, a large fraction of all the heteroatomic contacts, spread fairly uniformly over about twice as large a range, 3.36−3.61 Å, or 0.25 Å, seemingly reflecting both a more flexible positioning of Ca about the more constrained Cd/Pt framework and a rather uniform packing of the whole structure itself. In distinct contrast, the more delocalized Cd−Cd bonding distances exhibit a large range, 0.37 Å, for 2.81−3.18 Å.

Structures of Other Cd-Rich Phases. This is the first observation of Cd_7 PBP clusters as well as pronounced Cd aggregation with such short Cd−Cd bonds. Generally, less Cd in the form of separate Cd_4 tetrahedra occurs in Au- or Pt-richer intermetallics in which polar bonding with d-element components dominate, for example, in $La_{23}Pt_7Cd_4$[34] and Gd_4PtCd[35] (Cd−Cd: 3.17 Å and 3.19−3.25 Å, respectively). Also, tetrahedral star clusters, in which the faces of an inner Cd_4 tetrahedron are capped by Cd in a larger tetrahedron (Cd_4@Cd_4), occur in the Cd-richer $Na_6Au_7Cd_{16}$[16] (d(Cd−Cd) = 3.08−3.30 Å), $Ca_6Pt_8Cd_{16}$,[23] and others, again with generally strong bonding in the presence of a greater fraction of d-elements. Some examples of alkaline-earth−cadmium systems show pronounced, even complete, mixing of Au and Cd atoms on common lattice sites, which makes them less useful indicators of the Cd chemistry; for example, in $Ca_5Au_{10}Cd_2$ (of the $Ca_4Au_{10}In_3$ type[36]) and $Ca_{11}Au_{4-x}Cd_{18+x}$ ($x \leq 0.6$, see below).[37] The entire structure of the last phase, with roughly twice the Au:Cd proportion as Pt:Cd in Ca_6PtCd_{11}, is just a variant of the alternately facing Pt-capped Cd_4 rings (Figure 1c), namely, chains of pairs of puckered Cd_6 rings above and below gold apexes. In the Cd-rich binary phase $BaCd_{11}$, the basic building units are Cd_4 tetrahedra that share trans edges to form puckered chains.[38]

A few unusual alkali metal−cadmium intermetallics are known, and the complex and puzzling $Na_{26}Cd_{141}$[39] with 20 independent atoms is probably the most noteworthy. This is close in composition to Na_2Cd_{11}[40] (of the Mg_2Zn_{11} type) but with high coordination numbers typical of an intermetallic system in a layered hexagonal structure. However, the phase does not seem to have been well studied or perhaps even verified. There is also some concern because the phase is reportedly metastable with respect to Na_2Cd_{11} and must be quenched to be isolated; impurity stabilization may be involved. A superstructure result has recently been discovered as a partial clarification of a second mysterious phase $K_{0.37}Cd_2$,[39] an almost commensurately modulated tetragonal tunnel structure K_3Cd_{16} (*P4/nnc*)[41] that is somewhat similar to that of $Na_{0.72}Au_2Zn_2$.[17]

Separate families of much more complex *aperiodic quasi*crystals (QCs) have been discovered in related systems in recent decades, and these are also accompanied by characteristic and more conventional *periodic approximants* (ACs) that can be analyzed by conventional crystallographic means.[42] Ca−Cd examples of QCs are well-known, including the quite famous $CaCd_{5.75}$, one of the first two *binary* quasicrystals, $YbCd_{5.7}$ being the other.[43] The corresponding MCd_6 AC phases in the well-known YCd_6 structure type ($Im\bar{3}$)[44] are their so-called 1/1 crystalline approximants. However, the AC structures of this (see Tsai[43]) and other types are in each group nearly all the same and quite different from those we have been considering; namely, multiply endohedral in a sequence from the center outward of a tetrahedron (4), a pentagonal dodecahedron (20), an icosahedron (of cations; 12), an icosidodecahedron (30), and so on, and their e/a values are small (~2) and within a limited range. The different expressions of 5-fold symmetry in the numerous pentagonal bipyramids in the present Ca_6PtCd_{11} led us to consider these as possible forecasts of something new among the so-called decagonal (2D) quasicrystal family and their approximants.[45] For these reasons, we ran exploratory reactions over a range of Ca−Cd−M compositions for M = Pt, Pd, Au and valence electron concentrations (VEC) = 1.90−1.78 e, but no evidence for any new or suggestive quasicrystalline or approximant phase was found.

Electronic Structure and Chemical Bonding. These results pinpoint several unusual characteristics of Ca_6PtCd_{11}. The calculated electronic densities of states (DOS) for all atom types in Ca_6PtCd_{11} as well as for the different orbital types on each element are shown as a function of energy in Figure 4a−d. The COHP data for the nearer neighbor Ca−Ca, Ca−Cd, Ca−Pt, Pt−Cd, and Cd−Cd interactions both per average bond and per cell are shown in Figure 4 e and f, respectively. The corresponding weighted integrations of the last, the ICOHP (Hamilton population) results, are summarized for pairs of atom types in Table 3 and in individual detail with distances in Supporting Information, Table S2. These data presumably

dx.doi.org/10.1021/ic401455c | *Inorg. Chem.* 2013, 52, 10112−10118

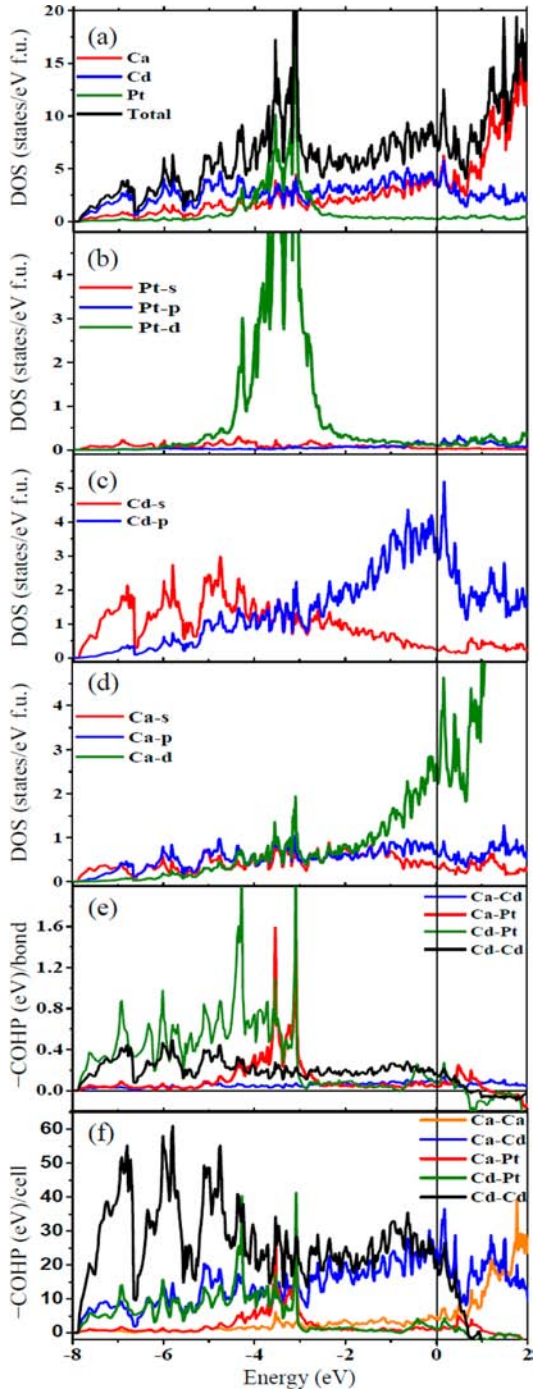

Figure 4. Results of LMTO-ASA calculations for $Ca_6Cd_{11}Pt$ cell considering Cd 4d as the core. (a) DOS for different atom types. (b) Partial projections of orbital components Pt 5d, 6s, 6p. (c) Cd 5s, 5p. (d) Ca 4s, 4p, 3d. (e) −COHP values in eV per average bond and (f) in eV per cell for Ca−Ca (orange), Ca−Cd (blue), Ca−Pt (red), Cd−Pt (green), and Cd−Cd (black) interactions.

provide better measures of the separate bonding interactions than do the corresponding distance measures, and they also highlight some novel features.

Substantial numbers of Cd 5p and Ca 3d states at E_F presumably ensure open states at that point and thence metallic characteristics for Ca_6PtCd_{11} (VEC = 34 e; e/a = 1.89). Although there is a pseudogap at a VEC of 39 e, about 0.6 eV or 5 e^-/f.u. higher, a few attempts to achieve a new phase near

Table 3. Bond Length Ranges and ICOHP Values for Average Bonds of Each Type in $Ca_6Cd_{11}Pt$ (Per Bond and Per Cell)

bond	length (Å)	−ICOHP (eV/per bond)	n/cell	−ICOHP (eV/cell)	%
Cd−Pt	2.795(1)-2.799(1)	1.46	16	23.4	8.06
Cd−Cd	2.807(1)-3.179(1)	1.07	124	133	45.8
Ca−Cd	3.358(2)-3.761(2)	0.40	264	105	36.4
Ca−Pt	2.887(2)-3.204(1)	0.94	20	18.8	6.49
Pt−Pt	3.532(1)	0.14	4	0.64	0.22
Ca−Ca	3.603(2)-3.940(3)	0.17	52	8.84	3.05

that point through complete or partial substitutions of related electron-richer elements (e.g., Y or Au) did not yield anything that was obviously new. In general, searches of diverse systems for composite or new structures near such pseudogaps through simple substitutional tunings have not been productive, suggesting that new structures at these points may either be unique and much too individualistic for such simple tuning efforts or be nonexistent.

Some significant chemical bonding features can be judged to some extent from the DOS and COHP curves and the ICOHP values therefrom. As experience teaches us, the more atypical Cd−Pt bonding in Ca_6PtCd_{11} affords the largest ICOHP population *per bond* (mol.), 1.46 eV, but this feature occurs infrequently and contributes only 8% of the total population *per cell* (Table 3) (and something of that magnitude to phase stability as well, ignoring details of the unknown decomposition products). The Ca−Pt interactions (20/cell; Figure 3b) are likewise quite specific but few in number and constitute only 6.5% of the ICOHP total. In notable contrast, the 124 nominally nonpolar Cd−Cd contacts average a substantial 1.07 eV *per bond*, which in composite make these contributions to ICOHP per cell the largest among all bond types, 45.8%. Even so, more than twice as many Ca−Cd as Cd−Cd contacts boost the smaller average bond population of the former, 0.40 eV/bond.mol, to make the Ca−Cd total the second largest per cell, 36%. The strikingly different character of the remaining Ca−Ca covalent assessments, both fewer (52) and numerically smaller (0.17 eV/bond), contribute only at the 3% level overall, another unusual feature of this particular interaction.

Generalities. More attention to the characters of the orbital contributions in the present compound is informative and helpful. The somewhat separate contributions of the Cd 5s and 5p states to the DOS as a function of energy become more distinctive as major amounts of a d element are not involved (Figure 4c[16,23]). The degree to which the Cd−Cd 5s and 5p interactions constitute a majority of the total COHP per cell over the entire bonding region is noteworthy, with lesser values from Pt 5d, 6s−Cd in the lowest energy region and Pt 5d−Ca 3d over the intervening −5 to −3 eV region (Figure 4f). The large COHP contribution of host Cd−Cd bonding (black, mostly 5s) at the lower energies is most striking, and this is followed by a continued increase from Cd 5p to near E_F (in concert with Cd DOS, Figure 4c). The distinctively smaller relative contributions of Ca 4s, 4p to DOS over all regions, presumably in a more cationic role, is also noteworthy relative to the effects of about twice as much Cd (Figure 4, panel d versus panel c). The results of the more numerous but smaller

dx.doi.org/10.1021/ic401455c | *Inorg. Chem.* 2013, 52, 10112−10118

Table 4. Cd−Cd Distances and Associated ICOHP Values Per Formula Unit for Some Cadmium-Rich Ternary Compounds

phases	Cd−Cd distances	−ICOHP[a] (eV/bond)	Cd−Cd bonds/f.u.	Cd−Cd coordination number	reference
$BaPt_2Cd_4$ $P4_2/mnm$, $Z = 2$	2.997−3.090	0.88−0.71	12	6	23
$Ca_3Pt_4Cd_8$ $Fm-3m$, $Z = 4$	3.031−3.242	0.71−0.36	24	6	23
$Na_6Au_7Cd_{16}$ $Fm-3m$, $Z = 4$	3.078−3.303	0.66−0.33	48	6	16
Ca_6PtCd_{11}, $Pnma$, $Z = 4$	2.807, 2.899−3.087, 3.179	1.75, 1.30−0.81, 0.41	1, 29, 1	6.6_{aver}	this work
Cd metal ($P6_3/mmc$, $Z = 2$)	2.977−3.291	0.99−0.47	6	12	47
hexagonal $CaCd_2$ ($P6_3/mmc$; $Z = 4$)	2.939−3.058	1.22−0.75	6	6	48
orthorhombic $CaCd_2$ ($Imma$; $Z = 4$) HT	2.850−2.932	1.48−1.27	4.5	4	25
Na_2Cd_{11}	2.846−3.466			9−12	40
$BaCd_{11}$	2.922−3.297			10−12	38

[a]ICOHP values are not quantitatively comparable between different phases.

COHP values for Ca 3d−Cd 5p (Figure 4, blue, in the character of back-donation to a cation) also follow the major Cd−Cd bonding above about −3 eV and continue in lesser amounts to about −8 eV along with Cd (5s)−Pt (5d, 6s) (Figure 4, green). Strikingly, only Cd−Cd (Figure 4, black) and Ca−Cd (Figure 4, blue) contribute to bonding above the Pt 5d levels, Cd−Cd remaining bonding beyond E_F to ∼0.8 eV, whereas Ca−Cd shows a pseudogap at ∼0.6 eV (+5e⁻/f.u.) but continues as bonding well above. These states are of course empty, but their character might be regarded as manifestations of some degree of unfulfilled bonding.

The behavior and state of Ca in this compound also warrant some collective considerations. An earlier note was made of the smaller sizes and narrower distribution of Ca−Ca distances in the structure, the separations ranging over only 0.14 Å and with values 8% below twice Pauling's r_{12} metallic radius, in contrast to other distance types. The corresponding ICOHP (covalency) for Ca−Ca is quite small, only 3% of the total per cell. Also, Ca DOS characteristics as an active metal relative to Cd show relatively little 4s, 4p participation but pronounced Ca 3d involvement above about −2 eV. The corresponding Ca−Ca COHP data, the orange curve in Figure 4f, parallel this, marking the Ca 3d participation in bonding to Cd and Pt already noted, the former extending in small measure to E_F. Ca−Ca, Ca−Cd, and Cd−Cd all exhibit appreciable numbers of virtual states at and above that point. Earlier LMTO calculations on related compounds of alkaline-earth[23] and rare-earth metals[46] suggest that the valence s and p levels similarly increase in energy whereas valence d states fall on oxidation of the active metals. These foregoing characteristics as well as the differences in the Mulliken electronegativities suggest that an appreciable degree of ionization of calcium in this phase would be consistent with all of the results.

The substantial and broad contributions of all Cd valence orbitals when that element is present in large proportions should be remembered, especially in instances without large contributions (or competition) from d elements or cations. Overall, the major Cd−Cd and then Ca−Cd bonding contributions in the COHP around the Fermi level are substantial (Figure 4f), whereas the strong Pt−Cd effects are substantial only in the Pt-richer ternary phases (Table 4). These trends should be capitalized on. Little attention has been paid to the limited number of somewhat divergent intermetallic compounds of cadmium, and some intercomparisons among their Cd−Cd distances and ICOHP data per f.u. are useful.

In Table 4, the Ca_6PtCd_{11} data stand out. As already noted, the first three phases listed in Table 4 incorporate substantial amounts of Pt or Au, and the effect of their stronger bonding (larger ICOHP values) in these phases with Cd is evident in the reduced Cd−Cd values, even though the Cd−Cd coordination numbers remain at 6. A number of very different circumstances with Ca_6PtCd_{11} has already been noted and discussed, but Ca_6PtCd_{11} also affords interesting contrasts with the three simpler examples that follow, hexagonal Cd metal[47] and the two $CaCd_2$ phases,[25,48] the hexagonal close packed version at room temperature, and an orthorhombic polytype that is stable at room temperature only when quenched. The ICOHP datum for cadmium metal looks distinctly inferior until the amount of metal is doubled in order to compare the same amount of Cd−Cd data for $CaCd_2$. However, the latter are in effect diluted by Ca, but the phase gains through additional Ca−Cd terms, so these two are not directly comparable. However, the relationship between the two $CaCd_2$ phases is clearer than before regarding the need to quench the high-temperature form. These data show that the latter appears to be a more typical high-temperature phase, with fewer Cd−Cd bonds per cell and presumably a higher entropy as well. It was noted in the Experimental Section that Ca_6PtCd_{11} also produces the same high-temperature phase (and unknowns) when quenched from 900 °C, the reverse transition being above 600 °C.

■ CONCLUSIONS

The new trail-breaking compound Ca_6PtCd_{11} has been synthesized, and its structural and bonding properties have been investigated. This unusual phase features an unprecedented degree of cadmium aggregation, including linear chains, novel Cd_7 PBP aggregates, and edge-shared chains of $PtCd_{4/2}$ square pyramids. Manifestations of this chemistry elsewhere have evidently been precluded in earlier work by the inclusion of larger amounts of the strong d-metal bonding Au or Pt. Under the right conditions Cd seems quite effective as an open s,p-band metal. But we remain woefully unequipped to predict such novel unknown structures on a firm basis, let alone new examples of known structures, and so discovery must still lead the way.

■ ASSOCIATED CONTENT

Supporting Information

Tables of anisotropic thermal displacement parameters, bond distances, and corresponding ICOHP values for Ca_6PtCd_{11}; powder X-ray diffraction data; the complete COHP plot; neighboring atom polyhedron for all independent atoms in Ca_6PtCd_{11}; cif files.This material is available free of charge via the Internet at http://pubs.acs.org.

AUTHOR INFORMATION

Corresponding Author

*E-mail: jdc@ameslab.gov.

Present Address

[†](F.G.) Department of Chemical Education, Sriwijaya University, Inderalaya, South Sumatra, Indonesia.

Notes

The authors declare no competing financial interest.

ACKNOWLEDGMENTS

F.G. acknowledges the support of the Fulbright Scholar Program. Qisheng Lin helped guide our searches for quasicrystalline analogues, and Gordie Miller provided useful theoretical insights and suggestions. The research was supported by the Office of the Basic Energy Sciences, Materials Sciences Division, U.S. Department of Energy (DOE). Ames Laboratory is operated for DOE by Iowa State University under contract No. DE-AC02-07CH11358.

REFERENCES

(1) Corbett, J. D. *Inorg. Chem.* **2010**, *49*, 13.
(2) Corbett, J. D. In *Chemistry, Structure, and Bonding of Zintl Phases and Ions*; Kauzlarich, S. M., Ed.; VCH Publishers: New York, 1996; Chapter 4.
(3) Corbett, J. D. *Angew. Chem., Int. Ed.* **2000**, *39*, 670.
(4) Miller, G. J.; Lee, C.-S.; Choe, W., In *Inorganic Chemistry Highlights*; Meyer, G.; Naumann, D., Wasemann, L., Eds.; Willey-VCH Verlag Gmbh: Weinheim, Germany, 2002; Ch. 2.
(5) Schäfer, H.; Eisenmann, B.; Müller, W. *Angew. Chem., Int. Ed.* **1973**, *12*, 694.
(6) Pyykkö, P. *Chem. Rev.* **1988**, *88*, 563.
(7) Liu, S. F.; Corbett, J. D. *Inorg. Chem.* **2004**, *43*, 4988.
(8) Li, B.; Corbett, J. D. *Inorg. Chem.* **2005**, *44*, 6515.
(9) Li, B.; Corbett, J. D. *J. Am. Chem. Soc.* **2006**, *128*, 12392.
(10) Li, B.; Corbett, J. D. *J. Am. Chem. Soc.* **2006**, *128*, 12392.
(11) Li, B.; Corbett, J. D. *Inorg. Chem.* **2007**, *46*, 6022.
(12) Dai, J. -C; Corbett, J. D. *Inorg. Chem.* **2007**, *46*, 4592.
(13) Smetana, V.; Corbett, J. D.; Miller, G. J. *Inorg. Chem.* **2012**, *51*, 1695.
(14) Smetana, V.; Miller, G. J.; Corbett, J. D. *Inorg. Chem.* **2012**, *51*, 7711.
(15) Lin, Q.; Corbett, J. D. *J. Am. Chem. Soc.* **2012**, *134*, 4877.
(16) Samal, S. L.; Corbett, J. D. *Inorg. Chem.* **2011**, *50*, 7033.
(17) Samal, S. L.; Lin, Q.; Corbett, J. D. *Inorg. Chem.* **2012**, *51*, 9395.
(18) Gupta, S.; Corbett, J. D. *Inorg. Chem.* **2012**, *51*, 2247.
(19) Gritner, K. D.; Schuster, H. U. *Z. Anorg. Allg. Chem.* **1994**, *620*, 1151.
(20) Hoffmann, R. D.; Pöttgen, R.; Dronskowski, R.; Landrum, G. A.; Kuennen, B.; Kotzyba, G. *Z. Anorg. Allg. Chem.* **1999**, *625*, 789.
(21) Stojanovic, M.; Latturner, S. E. *J. Solid State Chem.* **2007**, *180*, 907.
(22) Samal, S. L.; Corbett, J. D. *Z. Anorg. Allg. Chem.* **2012**, *638*, 1963.
(23) Samal, S. L.; Gulo, F.; Corbett, J. D. *Inorg. Chem.* **2013**, *52*, 2697.
(24) Zelinska, M.; Oryshchyn, S.; Zhak, O.; Pivan, J. Y.; Potel, M.; Tougait, O.; Noel, H.; Kaczorowski, D. *J. Solid State Chem.* **2010**, *183*, 2121.
(25) Bruzzone, G. *Gazz. Chim. Ital.* **1972**, *102*, 234.
(26) Schulze, G. E. R.; Wieting, J. *Z. Metallkd.* **1961**, *52*, 743.
(27) *WinXPow* 2.10, Stoe&Cie GmbH: Darmstadt, Germany, 2004.
(28) *SMART*, Bruker AXS, Inc.: Madison, WI, 1996.
(29) Blessing, R. H. *Acta Crystallogr.* **1995**, *A51*, 33.
(30) *SHELXTL*, BrukerAXS, Inc.: Madison, WI, 2000.
(31) Krier, G.; Jepsen, O.; Burkhardt, A.; Andersen, O. K. *TBLMTO-ASA Program*, version 4.7; Max-Planck-Institut für Festkörperforschung: Stuttgart, Germany, 1995.
(32) Jepsen, O.; Andersen, O. K. *Z. Phys. B: Condens. Matter* **1995**, *97*, 35.
(33) Dronskowski, R.; Blöchl, P. E. *J. Phys. Chem.* **1993**, *97*, 8617.
(34) Tappe, F.; Pöttgen, R. *Z. Naturforsch.* **2009**, *64b*, 184.
(35) Schappacher, F. M.; Rodewald, U. C.; Pöttgen, R. *Z. Naturforsch.* **2008**, *63b*, 1127.
(36) Lin, Q.; Corbett, J. D. *Inorg. Chem.* **2007**, *46*, 8722.
(37) Harms, W.; Dürr, I.; Röhr, C. *Z. Naturforsch.* **2009**, *64b*, 471.
(38) Sanderson, M. J.; Baenziger, N. C. *Acta Crystallogr.* **1953**, *6*, 627.
(39) Todorov, E.; Sevov, S. C. *Inorg. Chem.* **1998**, *37*, 6341.
(40) Wong, C. H.; Chieh, C.; Lee, T. Y. *Acta Crystallogr.* **1965**, *19*, 849.
(41) Mihajlov, V.; Röhr, C. *Z. Anorg. Allg. Chem.* **2010**, *636*, 1792.
(42) Pay Gómez, C.; Lidin, S. *Angew. Chem., Int. Ed.* **2001**, *40*, 4037.
(43) Tsai, A. P.; Guo, J. Q.; Abe, E.; Takakura, H.; Sato, T. J. *Nature* **2000**, *408*, 538.
(44) Larson, A. C.; Cromer, D. T. *Acta Crystallogr., Sect. B: Struct. Crystallogr. Cryst. Chem.* **1971**, *27*, 1875.
(45) *Quasicrystals: a Primer*, 2nd ed.; Janot, C., Ed.; Oxford University Press: Oxford, UK, 1992.
(46) Chai, P.; Corbett, J. D. *Inorg. Chem.* **2012**, *51*, 3548.
(47) Rossmanith, E. *Acta Crystallogr.* **1978**, *A34*, 497.
(48) Nowotny, H. N. *Z. Metallkd.* **1946**, *37*, 31.